CEST 2023

18th International Conference on Environmental Science and Technology

Athens, Greece, 30 August to 2 September 2023

Effects of High Temperature and Liquid Nitrogen Cooling: A Case Study of granite rocks from Kazakhstan

LONGINOS S.N.[1,*], TULEUGALIYEV M.[2], BEGALIYEV D.[1], HAZLETT R.[1]

[1]School of Mining and Geosciences, Department of Petroleum Engineering, Nazarbayev University, Astana 010000, Kazakhstan
[2]School of Engineering and Digital Sciences, Department of Chemical Engineering, Nazarbayev University, Astana 010000, Kazakhstan

*corresponding author: Sotirios Longinos
e-mail: sotirios.longinos@nu.edu.kz

Abstract Cryogenic fracturing using liquid nitrogen (LN_2) is a new geothermal well stimulation method to augment porosity, permeability, and overall contact area in Hot Dry Rock (HDR) reservoirs in an environmentally acceptable way, without potential surface or groundwater contamination, formation damage, and huge water consumption. Procedures representing different exposure times and frequencies were compared by investigating the degree of rock integrity damage created. Granite rocks equilibrated at different elevated temperatures from 200°C to 500°C were immersed in LN_2 for different freezing times (FT) and a variable number of freezing-thawing cycles (FTC). Rock strength was measured in compression tests. Scanning electron microscopy (SEM) was used to confirm the extent of visible damage and catalog the fracture evolution of our granite specimens. Two different granite rocks were studied: Zhylgyz (sample 1) and Sayac (sample 2). The experiments document mechanical rock damage by thermal shock and the degree of thermo-fracturing rises with temperature difference and time of LN_2 treatment in both freezing time and freezing-thawing cycle methods.

Keywords: Granite, Kazakhstan, Liquid nitrogen, Geothermal Energy

1. Introduction

Energy transition refers to moving from fossil-based energy to renewable-based systems [1-4]. Hot Dry Rocks (HDR) have been identified as a potential future renewable source and an alternative to traditional fossil fuels. HDRs are located at 2 to 10km depths, corresponding to the viable process temperature range of 150 to 650°C [5-8]. Extraction of heat from hot dry rocks ensures clean and highly efficient energy conversion. Typically, HDRs are impermeable formations, and thus, it is required to create a network of interconnected fractures to provide a conduit for heat extraction and thermal energy production. In such enhanced geothermal systems (EGS), a fracturing medium must establish connectivity between injection and production wells [9,10]. Many countries with HDR reservoirs consider expanding their share of geothermal energy in their overall energy consumption. China and other South Asian countries aim to lead in geothermal energy production [11,12].

Today, hydraulic fracturing is considered as one of the most widespread methods of fracturing due to its effectiveness in economic terms [13]. The injection of a cold-water jet in HDR initiates thermal shock, resulting in rock strength diminution and induced cracking. Besides the limitations of hydraulic fracturing, including excessive water consumption and contamination, only one massive fracture is typically generated [14-16]. Therefore, waterless techniques increase effectiveness and lower the environmental impact. As an alternative, liquid nitrogen (LN_2) can be used as the fracturing liquid instead of water. The extremely low temperature of LN_2 (−196°C at atmospheric conditions) creates very high thermal stresses and degrades rocks severely [16,17]. In this research, the effect of the cryogenic fracturing process is observed on two different granite types. The granite's axial stress and absorbed energy after LN_2 exposure were investigated. Along with these, the surface of the granite samples was investigated using scanning electron microscopy (SEM). Samples were tested for the impact of different initial temperatures and two different procedures related to the contact or freezing time (FT) and the number of thermal shocks plus relaxation (thawing) cycles (FTC).

2. Materials and experimental process

Granite samples were gathered from outcrops from different regions of Kazakhstan. Two kinds of granite known as “Zhylgyz (sample 1)” and “Sayac (sample 2)” were used. Cylindrical cores were cut from the base material. Each sample was 50mm in length and 2mm in diameter. Before testing, specimens were set in a drying oven for 1 hour at 50°C. Then, there were two different experimental procedures. In the freezing time (FT) process, separate specimens were placed in a heating furnace at 200°C, 300°C, and 500°C, respectively, for 2 hours and then plunged in LN_2 of cooling for 1 hour, followed immediately by analyses. In the freezing-thawing cycle (FTC) process, after 2 hours of heating, granite samples were immersed in LN_2 for 5 minutes and then exposed to environmental conditions for 5 minutes, completing one cycle. The freezing and thawing processes were repeated for 10 cycles (C10) or 20 cycles (C20). All samples were subjected to compression strength testing, supported by acoustic emission recording immediately upon process completion. Last, for those samples initially subjected to 300oC and 500^{o}C from both processes, specimens were examined using scanning electron microscopy (SEM) on a JSM-IT 200 to describe the progression of fractures evident from external surfaces. Figure 1 shows the experimental process.

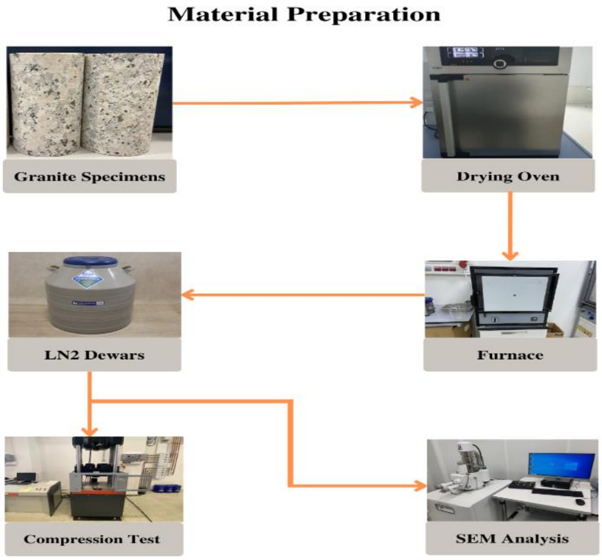

Figure 1. Experimental process and devices

3. Results and discussion

3.1. Compression tests

Uniaxial compression tests were carried out to measure the strength of processed granite samples and to observe how the granite sample distorted under particular experimental conditions compared to untreated specimens. Figures 2, 3, and 4 show stress versus time for the freezing time process and the two freezing-thawing cycle processes (C10 and C20), respectively, utilizing two different granite types.

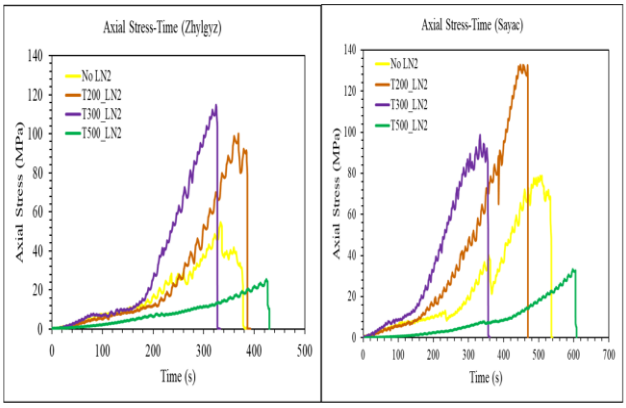

Figure 2. Axial Stress versus Time after LN$_2$ treatment for three different heating temperatures for Zhylgyz (left), Sayac (right) granite samples

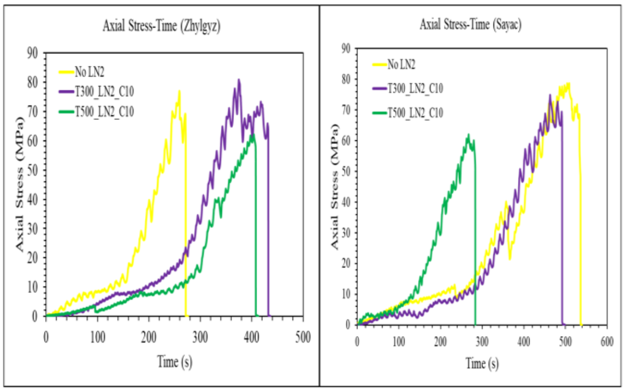

Figure 3. Axial Stress versus Time after LN$_2$ treatment with 10 freezing-thawing cycles for 2 different heating temperatures for Zhylgyz (left), Sayac (right) granite samples.

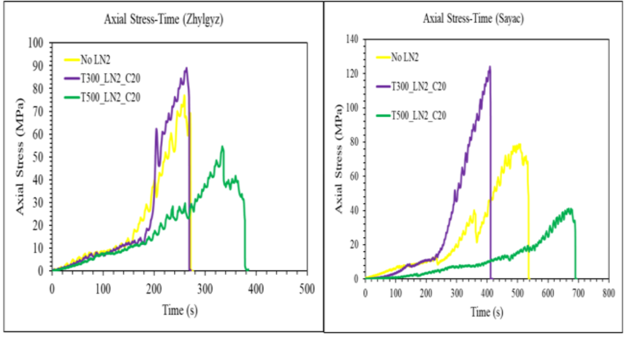

Figure 4. Axial Stress versus Time after LN$_2$ treatment with 20 freezing-thawing cycles for 2 different heating temperatures for Zhylgyz (left), Sayac (right) granite samples.

As shown in Figure 2 for the freezing time process and summarized in Table 1, the axial stress peak is highest in the Sayac granite experiment with maximum value 132.5MPa for an initial temperature of 200^{o}C. In the Zhylgyz sample, the maximum axial stress occurred in the 300^{o}C experiment with a value of 114.6MPa. Comparing baseline granite specimens and specimens with heating and cooling procedures, there is only a reduction in axial stress in tests with heating at 500^{o}C, 57.7% for Sayac, and 66.9% for Zhylgyz.

In Figure 3, which captures the results of experiments with 10 freezing-thawing cycles, the maximum peak uniaxial compression strength (UCS) was found in the experiment preheated to 300^{o}C for Zhylgyz with values of 80.9MPa. In Sayac experiments, the highest value of peak UCS was in the baseline sample without any LN$_2$ treatment at 78.7MPa, slightly higher than in the 300^{o}C trial with a value of 74.9MPa. Like FT procedures, freezing and thawing cycles also revealed reductions in axial stress only in specimens preheated to 500^{o}C, exhibiting reductions of 21.2% for Sayac and 19.3% for Zhylgyz. It should also be noted that in studies with 10 freezing-thawing cycles preheated to 500^{o}C, the reduction in peak UCS, while apparent, is not significant concerning other heating settings. This demonstrates that the freezing-thawing process has a minor deleterious impact.

In Figure 4, for 20 freezing-thawing cycle experiments, the most significant results were recorded for granite warmed to 300^{o}C, namely, 124MPa for Sayac and 89MPa for Zhylgyz. Compared with baseline granite samples, there is a decline in axial stress only in samples heated to 500^{o}C, with percentage reductions of 47.8% for Sayac and 38.8% for Zhylgyz. With granite heated to 300^{o}C and 20 freezing-thawing cycles, UCS values are somewhat higher than in experiments with no LN$_2$ treatment in all three samples. Samples heated to 500^{o}C and then subjected to either 10 or 20 freezing-thawing cycles produce smaller UCS values. This phenomenon occurs when minerals heated to greater temperatures face greater thermal stresses, resulting in more deformity. The properties of quartz, as a major constituent, have a big impact on thermally induced failure. It should also be noted that quartz has a greater thermal expansion value than other minerals. Moreover, there is a clear distinction between freezing time and freezing-thawing cycle trials in that freezing time experiments show lower UCS peak values. This is the opposite result obtained using coal, where frost forces were found to create fissures and crevices that enhance the permeability of samples and make samples weaker compared to their initial situation.

3.2. SEM analysis

Scanning electron microscopy (SEM) confirmed structural damage in the two granite types subjected to the various LN$_2$ treatments of freezing time and freezing-thawing cycles. The outcomes are presented in Figures 8 and 9. For the Zhylgyz sample, after 60 minutes of freezing, the generation of thermally induced cracks or observation of the expansion of preexisting fractures was noticed on the granite surface, as depicted in Figure 8. One microfracture with a length of 18 micrometers was created after LN$_2$ treatment. The width of this fracture does not exceed 500 nanometers. The enlargement of preexisting fractures is quite modest, and the growth of only a few hundred nanometers can be detected. Overall, there were little changes in the granite structure after 60 minutes of freezing.

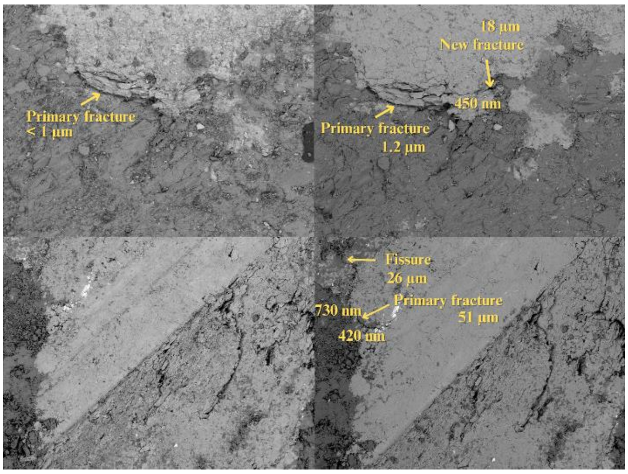

Figure 8. SEM analysis of Zhylgyz for freezing time (left top and right top) and freezing-thawing cycles (left bottom and right bottom)

After 10 cycles of LN$_2$ freezing and thawing, visible changes on the granite surface are observed, as shown in Figure 8. A long primary fracture of 51 micrometers was produced, undergoing thermal shock. The width of this fracture ranged from 400 to 800 nanometers. Moreover, close to this fracture, another thinner crack (fissure) was developed with a width of less than 400 nanometers. The length of the fissure is 26 micrometers. These newly formed cracks surely increase the sample permeability. Compared to a freezing time of 60 minutes, 10 cycles of freezing and thawing is much more efficient for improving sample permeability if microcracks hold such evidence.

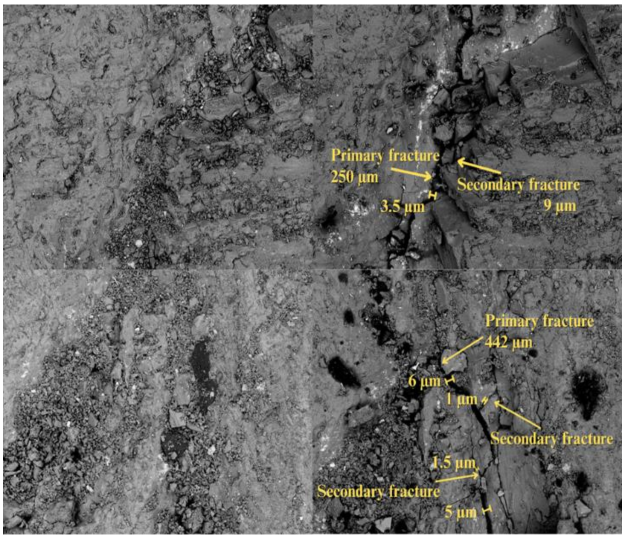

Figure 9. SEM analysis of Sayac for freezing time (left top and right top) and freezing-thawing cycles (left bottom and right bottom)

For the Sayac granite sample illustrated in Figure 9, after 60 minutes of freezing, the formation of a massive main fracture crossing the whole observation area is noticed. The length of this fracture is 250 micrometers, while the width is 3-5 micrometers along the whole fracture. In addition, secondary fractures were formed after LN$_2$ treatment but with a length of only a few micrometers. The width of a secondary fracture is about 2-3 micrometers. As a result, creating primary and secondary fractures creates a fracture network that may provide high conductivity and permeability for granite. Moreover, it is important to note that fractures originate at mineral boundaries.

For the Sayac sample exposed to the freezing-thawing cycle process, a primary fracture appeared with a maximum aperture size reaching 6 micrometers, as depicted in Figure 9. The length of this primary fracture was 442 micrometers. Connected to the primary fracture, many secondary fractures were formed, creating fracture networks with widths of less than 1 micrometer, 1, and 1.5 micrometers. A Y-shaped fracture network can be observed on the granite surface. The thermal effects caused by LN$_2$ in the fracturing process may assist in pressure reduction, generating an enhanced-permeability region. The thermal stresses affected and weakened granite structure integrity, creating intergranular cracks due to freezing-thawing cycles.

Generally, the most substantial modification changes were observed in Sayac granite, where no fractures were noticed before LN$_2$ treatment. After LN$_2$ exposure, primary and secondary fractures produced Y-shaped fracture networks. For Zhylgyz granite, changes are less dramatic, with no indication by SEM of fracture network formation.

4. Conclusion

To investigate the influence of environmentally acceptable LN$_2$ cooling on the failure of heated granite, we conducted a series of physical and mechanical tests from two different granite sources from Kazakhstan. Microstructures of the granites cooled with LN$_2$ are also noticed to reveal the characteristics and contingent mechanisms of thermal failure. The primary outcomes are presented below:

1) Smaller values in UCS peaks resulted in all experiments pre-equilibrated at 500°C before exposure to LN_2.
2) Samples pre-equilibrated at 500°C and exposed to LN_2 for a longer time showed the largest augmentation in measured permeability.
3) The two granites examined behaved similarly regarding compressive strength and followed similar trends regarding the impact of the initial temperature; however, the sensitivity to thermally induced fracturing was varied, as indicated in the SEM examination.
4) Trends regarding the effect of initial granite temperature of 200°C and 300°C were reversed at severe temperatures, i.e., 500°C, possibly showing a shift in physical processes that influence a specimen's ability to preserve integrity after thermal shock at a threshold starting temperature or heal subsequently.

References

[1] Merey S., Longinos S. (2018), The role of natural gas hydrate during natural gas transportation. Ömer Halisdemir Üniversitesi Mühendislik Bilimleri Dergisi, **7(2)**, 937-953.

[2] Longinos S.N., Parlaktuna M. (2021), Kinetic analysis of arginine, glycine and valine on methane (95%)–propane (5%) hydrate formation. Reaction Kinetics, Mechanisms and Catalysis, **133(2)**, 741-751.

[3] Longinos, S.N., Parlaktuna M. (2021), Kinetic study of the effect of amino acids on methane (95%)—propane (5%) hydrate formation. Reaction Kinetics, Mechanisms and Catalysis, **133(2)**, 753-763.

[4] Longinos S.N., Longinou D.D., Celebi E., Toktarbay Z., Parlaktuna M. (2021), Kinetic study of methane hydrate formation with the use of a surface baffle. Reaction Kinetics, Mechanisms and Catalysis, **134**, 75-86.

[5] Longinos S.N., Parlaktuna M. (2021), Examination of asparagine, aspartic acid and threonine in methane (95%)-propane (5%) gas hydrates as kinetic inhibitors. Reaction Kinetics, Mechanisms and Catalysis, **134(1)**, 87-94.

[6] Zhang S., Huang Z., Zhang H., Guo Z., Wu X., Tianyu Wang, Zhang C., Xiong C. (2018), Experimental study of thermal-crack characteristics on hot dry rock impacted by liquid nitrogen jet. Geothermics, **76**, 253-260.

[7] Ruiyue Y., Huang Z., Shi Y., Yang Z., Huang P. (2019), Laboratory investigation on cryogenic fracturing of hot dry rock under triaxial-confining stresses. Geothermics **79**, 46-60.

[8] Wu X., Huang Z., Song H., Zhang S., Cheng Z., Li R., Wen H., Huang P., Dai X. (2019), Variations of physical and mechanical properties of heated granite after rapid cooling with liquid nitrogen." Rock Mechanics and Rock Engineering **52**, 2123-2139.

[9] Ge, Zhenlong, Qiang Sun, Tian Yang, Tao Luo, Hailiang Jia, and Duoxing Yang. (2021), Effect of high temperature on mode-I fracture toughness of granite subjected to liquid nitrogen cooling. Engineering Fracture Mechanics **252** ,107834.

[10] Ruiyue Y., Hong C., Liu W., Wu X., Wang T., Huang Z. (2021), Non-contaminating cryogenic fluid access to high-temperature resources: Liquid nitrogen fracturing in a lab-scale Enhanced Geothermal System." Renewable Energy **165**,125-138.

[11] S., Zhang, Huang Z., Huang P., Wu X., Chao Xiong, Zhang C. (2018), Numerical and experimental analysis of hot dry rock fracturing stimulation with high-pressure abrasive liquid nitrogen jet." Journal of Petroleum Science and Engineering **163**, 156-165.

[12] Ishida T., Aoyagi K., Niwa T., Chen Y., Murata S., Chen Q., Nakayama Y. (2012), Acoustic emission monitoring of hydraulic fracturing laboratory experiment with supercritical and liquid CO2. Geophysical Research Letters, **39**(16).

[13] Anderson R.L., Ratcliffe I., Greenwell H.C., Williams P.A., Cliffe S., Coveney P.V. (2010), Clay swelling—a challenge in the oilfield. Earth-Science Reviews, **98(3-4)**, 201-216.

[14] Sheremetov L., Cosultchi A., Martínez-Muñoz J., Gonzalez-Sánchez A., Jiménez-Aquino M.A. (2014), Data-driven forecasting of naturally fractured reservoirs based on nonlinear autoregressive neural networks with exogenous input. Journal of Petroleum Science and Engineering, **123**,106-119.

[15] Zhang, D., Tingyun, Y. (2015), Environmental impacts of hydraulic fracturing in shale gas development in the United States. Petroleum Exploration and Development, **42(6),** 876-883.

[16] Alqatahni, N.B., Cha, M., Yao, B., Yin, X., Kneafsey, T.J., Wang, L., Wu, Y.S. and Miskimins, J.L. (2016), Experimental investigation of cryogenic fracturing of rock specimens under true triaxial confining stresses. In SPE Europec featured at 78th EAGE conference and exhibition. OnePetro.

[17] Cai C., Huang Z., Li G., Gao F., Wei J., Li, R. (2016), Feasibility of reservoir fracturing stimulation with liquid nitrogen jet. Journal of Petroleum Science and Engineering, **144,**59-65.